Chapter 9
Analysis and Test Research for Three-Phase Short-Circuit of Permanent Magnet Synchronous Motor for an Electric Vehicle

Sibo Wang, Chao Lu, Xiaoxu Wang and Huichao Zhao

Abstract Permanent magnet synchronous motor (PMSM) is widely used in the electric vehicle as a drive motor. For specific application requirements of the electric vehicle motor system, there are new faults and application characteristics in motor system's three-phase short-circuit. Based on the *dq* axis coordinate system mathematical model of PMSM, this paper derives the *dq* axis current transient equations of three-phase transient short-circuit with load or without load in initial state. Combined electric vehicle PMSM operating characteristics, based on the typical working conditions, this paper analyzes the influences of motor demagnetization risk in different conditions by comparing the transient current changing process simulation results of different initial transient *dq* axis currents. Then according to the characteristics of the three-phase transient short-circuit, designs and builds a test platform, and verifies the correctness of the analysis and mathematical simulation models by testing. It provides an important theoretical analysis and test verification methods for analyzing the electric vehicle PMSM three-phase short-current function and determining the risk of demagnetization.

Keywords Electric vehicle · PMSM · Three-phase transient short-circuit · Transient short-circuit test

9.1 Introduction

Electric vehicles is an important developing trend to cut off emission, nowadays, mainstream OEMs have invested heavily for this kind of future vehicles. Permanent magnet synchronous motor (PMSM) which has been widely used in the electric

S. Wang (✉) · C. Lu · X. Wang · H. Zhao
E-motor system development Sec., Electric Vehicle Dept.,
FAW R&D Center, Changchun, China
e-mail: wangsibo@rdc.faw.com.cn

© Springer Nature Singapore Pte Ltd. 2017

Society of Automotive Engineers of China (SAE-China), *Proceedings of SAE-China Congress 2016: Selected Papers*, Lecture Notes in Electrical Engineering 418,
DOI 10.1007/978-981-10-3527-2_9

vehicle covers many advantages such as high torque and power density, wide range of flux-weakening control and easily maintenance. However, the PMSM system of the vehicle will also bring some new security features such as three-phase short-circuit. Research on three-phase short-circuit of traditional motor system has been done for years in China and abroad, but there are no literatures in-depth study of PMSM three-phase short-circuit for electric vehicles.

There are new fault handling and application characteristics on three-phase short-circuit in the field of electric vehicles. On the one hand, the three-phase short-circuit as a kind of fault may cause the demagnetization of permanent magnets or partial demagnetization [1]. The rising winding temperature and vibration noise caused by short-circuit may lead to the damage of other parts of the vehicle. On the other hand, if critical fault such as the inverter IGBT breakdown or insulation failure on high voltage system happens suddenly during the vehicle moving, the inverter can execute a three-phase active short-circuit to decouple the motor and transmission system in order to avoid the risk of the motor over-speed. This function can guarantee that the inverter thin-film capacitor and power devices are not be broken down by over voltage and also can braking the vehicle and shut down the engine safely by the anti-drag torque [2]. The three-phase short-circuit may be either one kind of fault or one kind of active safety function. The vehicle configurations, motor electromagnetic and heat dissipation solutions, and the safety requirements for electronic control system are all needed to be considered as a safety function. Above all, the three-phase short-circuit condition analysis is crucial for electric vehicles' safety.

Before designing a three-phase active short-circuit function or analyzing the failure modes of the system after three-phase short-circuit, it should be confirmed that there is no risk of reversible demagnetization at the condition of three-phase transient short-circuit. Considering the maximum negative -axis current when the motor working, the demagnetization current limit and safety factor should be set during the design, but there is no security check for motor transient short-circuit conditions [3]. Thus, it is necessary for electric vehicle motor design to analyze the negative-axis current at the three-phase transient short-circuit condition and confirm the current within the maximum range of the demagnetization current by testing. Electric vehicle drive system increases the new motor system, which has different degrees of coupling relationship with engine, transmission and so on as a new source of power. Since the working condition is extremely complex, the motor is usually designed as high output and wide speed range in order to match the power train system. When we are analyzing the three-phase transient short-circuit, the vehicle condition such as low speed start, driving generating etc. shall be considered to evaluate the effect caused by the transient short-circuit demagnetization current. The three-phase transient short-circuit test platform and research method is aimed at steady state or low power permanent magnet synchronous motor [4]. There is a problem of transient test bench speed fluctuation caused by the transient impact [5]. Then to simulate electric vehicle short-circuit condition on the bench, it is worth to study how to solve the speed fluctuation problem caused by three-phase transient short-circuit and ensure the safety of the system and dynamic synchronous sampling.

Based on the *dq*-axis model of vector control, this paper derives the *dq*-axis current equations of the electric vehicle motor system at the time of three-phase transient short-circuit. And based on different initial working conditions, this paper analyzes the condition where the maximum demagnetization current occurs during the three-phase transient short-circuit. This paper also gives out the simple simulation algorithm to verify the maximum demagnetization current, and verifies the correctness of the transient short-circuit current equations through the test.

9.2 Three-Phase Transient Short-Circuit Model

Usually, the short-circuit current's curve change over time can be calculated by CAE simulation software in engineering design. In this paper, the process of PMSM transient short-circuit can be analyzed by vector control of the *dq*-axis model, which can be used to analyze the steady-state and transient process. The algorithm also has a salient feature that is fast operation and evaluation.

Before establishing the mathematical model, the follow assumptions shall be done.

(1) Ignore the rotor core reluctance, excluding the eddy current and hysteresis loss.
(2) The conductivity of permanent magnet material is zero, and the magnetic permeability inside the permanent magnet is consistent with the air.
(3) Permanent magnet excitation magnetic field generates a sine wave induced electromotive force in the phase windings.
(4) Permanent magnet magnetic field and three-phase armature reaction magnetic field is sinusoidal in the air gap.
(5) Ignore the effect of the magnetic saturation and the temperature to the motor parameters, the motor parameters are constant.

In this paper, interior permanent magnet synchronous motor (IPMSM) is used to establish a transient short-circuit model of permanent magnet synchronous motors. The model also applies to surface mounted permanent magnet synchronous motor (SPMSM). Interior permanent magnet synchronous motor's L_d and L_q is not equal. Currently, most vehicles with permanent magnet synchronous motor are interior, mainly because in the case of the same current, the output torque can be increased by the reluctance torque.

Figure 9.1 shows a synchronous rotating *dq*-axis, the U, V, W phase current is transformed into a stationary *dq*-axis current by the coordinate transformation. Voltage equation is given by

$$\begin{cases} U_d = R_S i_d + L_d \frac{di_d}{dt} - \omega_e L_q i_q \\ U_q = R_S i_q + L_q \frac{di_q}{dt} - \omega_e \left(L_d i_d + \psi_f \right) \end{cases} \tag{9.1}$$

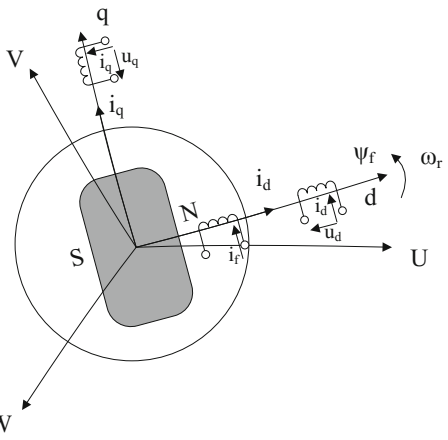

Fig. 9.1 Synchronous rotating *dq* axis

U_d, U_q	Stator voltage *dq*-axis component,
i_d, i_q	Stator voltage *dq*-axis component,
R_s	Stator phase resistance,
ψ_f	Flux linkage generated by permanent magnet,
$L_d L_q$	Stator winding *dq*-axis inductance,
ω_e	$\omega_e = p_n \times \omega_r, p_n$; Stator current electrical frequency,
p_n	Motor pole pairs,
ω_r	Rotor angular velocity.

Firstly, let's analyze the situation when *dq*-axis current is zero at the time of the three-phase short-circuit. The *dq*-axis transient short-circuit current and voltage is given by

$$\begin{cases} i_d(0_-) = 0, \quad i_q(0_-) = 0 \\ U_d(0_+) = 0, \quad U_q(0_+) = 0 \end{cases} \tag{9.2}$$

By Laplace transform the differential equations formula (9.1) can be transformed into complex frequency domain equation as (9.3).

$$\begin{cases} R_S i_d(s) + L_d s i_d(s) - \omega_e L_q i_q(s) = 0 \\ R_S i_q(s) + L_d s i_q(s) - \omega_e L_d i_d(s) + \psi_f = 0 \end{cases} \tag{9.3}$$

The formula (9.4) can be calculated by solving Eq. (9.3).

$$\begin{cases} i_q(s) = \dfrac{-\frac{r}{L_d L_q}\omega\psi_f - \frac{r}{L_q}\omega\psi_f s}{s\left(s^2 + s\left(\frac{r}{L_d} + \frac{r}{L_q}\right) + \frac{r^2}{L_d L_q} + \omega^2\right)} \\ i_d(s) = \dfrac{-\frac{1}{L_d}\omega^2\psi_f}{s\left(s^2 + s\left(\frac{r}{L_d} + \frac{r}{L_q}\right) + \frac{r^2}{L_d L_q} + \omega^2\right)} \end{cases} \tag{9.4}$$

The denominator can be decomposed into:

$$s\left(s^2+s\left(\frac{r}{L_d}+\frac{r}{L_q}\right)+\frac{r^2}{L_dL_q}+\omega^2\right)=s(s-s_1)(s-s_2)$$

where

$$s_1,s_2=-a\pm j\sqrt{b^2-a^2}=-\frac{r}{2}\left(\frac{1}{L_d}+\frac{1}{L_q}\right)\pm j\sqrt{\frac{r^2}{L_dL_q}+\omega^2-\frac{r^2}{4}\left(\frac{1}{L_d}+\frac{1}{L_q}\right)^2}$$

$$a=\frac{r}{2}\left(\frac{1}{L_d}+\frac{1}{L_q}\right),\quad b=\sqrt{\frac{r^2}{L_dL_q}+\omega^2},\quad c=-\frac{1}{L_d}\omega^2\psi_f$$

Solve the original function of the formula (9.5).

$$\begin{cases} i_d(s)=-\frac{1}{L_d}\omega^2\psi_f\frac{1}{s(s-s_1)(s-s_2)} \\ i_d(s)=\frac{c}{b^2}\begin{pmatrix}\frac{1}{s}-\frac{s+a}{(s+a)^2+b^2-a^2}\\ -\frac{a}{(s+a)^2+b^2-a^2}\end{pmatrix}\end{cases} \tag{9.5}$$

The original function is:

$$\begin{aligned} i_d(t)&=\frac{c}{b^2}\left[1-e^{-at}\begin{pmatrix}\cos\sqrt{b^2-a^2}\cdot t\\ +\frac{a}{\sqrt{b^2-a^2}}\sin\left(\sqrt{b^2-a^2}\cdot t\right)\end{pmatrix}\right] \\ &=\frac{c}{b^2}\left[1-\frac{b}{\sqrt{b^2-a^2}}e^{-at}\sin\begin{pmatrix}\sqrt{b^2-a^2}\cdot t\\ +\arctan\left(\frac{\sqrt{b^2-a^2}}{a}\right)\end{pmatrix}\right]\end{aligned} \tag{9.6}$$

Similarly

$$\begin{aligned} i_q(s)&=\frac{-\frac{r}{L_dL_q}\omega\psi_f-\frac{r}{L_q}\omega\psi_f s}{s(s-s_1)(s-s_2)}=-\frac{d}{b^2}i_d(s)-\frac{\omega}{L_q}\cdot\psi_f\cdot\frac{1}{(s-s_1)(s-s_2)} \\ &=-\frac{d}{b^2}i_d(s)-\frac{e}{b^2}\cdot\frac{b^2}{(s-s_1)(s-s_2)} \\ &=-\frac{d}{b^2}i_d(t)-\frac{e}{b^2}\cdot\frac{1}{\sqrt{b^2-a^2}}\cdot e^{-at}\sin\left(\sqrt{b^2-a^2}\cdot t\right)\end{aligned} \tag{9.7}$$

where

$$d=-\frac{r}{L_dL_q}\omega\psi_f,e=\frac{\omega}{L_d}\psi_f$$

The formula (9.7) is a transcendental function. The maximum $-i_d$ current cannot be calculated from this formula. But the response curve can be obtained by computer in engineering generally, so to obtain the maximum $-i_d$ current. This work will be described in detail in the next chapter.

$$\frac{c}{b^2} = -\frac{\omega^2 \psi_f L_q}{r^2 + \omega^2 L_d L_q}, \quad \frac{d}{b^2} = -\frac{r\omega\psi_f}{r^2 + \omega^2 L_d L_q} \tag{9.8}$$

Formula (9.8) are the steady-state final values of dq-axis current respectively, and are also the analytical expressions of the dq-axis steady-state short-circuit.

When the initial values of i_d, i_q is not zero, that is, the motor system has output torque at the time of transient short-circuit. The differential Eq. (9.1) has the following initial conditions.

$$\begin{cases} i_d(0_-) \neq 0, \quad i_q(0_-) \neq 0 \\ U_d(0_+) = 0, \quad U_q(0_+) = 0 \end{cases} \tag{9.9}$$

Solve the Laplace transform equations containing the initial value. The solution are:

$$\begin{cases} i_d(s) = \frac{i_d(0_-)\cdot s^2}{s(s-s_1)(s-s_2)} + \frac{\left[\frac{\omega_e L_q}{L_d} i_q(0_-) + \left(\frac{r}{L_q} - \frac{r}{L_d}\right) \cdot i_d(0_-)\right] \cdot s}{s(s-s_1)(s-s_2)} - \frac{\left[\frac{\omega_e r}{L_d} i_q(0_-) + \frac{\omega_e^2}{L_d}\psi_f + \frac{r^2}{L_d L_q} \cdot i_d(0_-)\right]}{s(s-s_1)(s-s_2)} \\ i_q(s) = \frac{i_q(0_-)\cdot s^2}{s(s-s_1)(s-s_2)} + \frac{\left[-\frac{r}{L_q} i_q(0_-) - \frac{\omega_e \psi_f}{L_q} + \frac{i_q(0_-)}{L_d r} - \frac{\omega_e L_d}{L_q}\right] \cdot s}{s(s-s_1)(s-s_2)} - \frac{\frac{\omega\psi_f r}{L_d L_q} + \frac{\omega r}{L_q} i_d(0_-)}{s(s-s_1)(s-s_2)} \end{cases} \tag{9.10}$$

The above formula can be written is given by

$$\begin{cases} i_d(s) = \frac{A\cdot s^2 + B\cdot s + C}{s(s-s_1)(s-s_2)} \\ i_q(s) = \frac{A'\cdot s^2 + B'\cdot s + C'}{s(s-s_1)(s-s_2)} \end{cases} \tag{9.11}$$

where

$$\begin{cases} A = i_d(0_-) \cdot s^2 \\ B = \left[\frac{\omega_e L_q}{L_d} \cdot i_q(0_-) + \left(\frac{r}{L_q} - \frac{r}{L_d}\right) \cdot i_d(0_-)\right] \\ C = \left[\frac{\omega_e r}{L_d} \cdot i_q(0_-) + \frac{\omega_e^2}{L_d}\psi_f + \frac{r^2}{L_d L_q} \cdot i_d(0_-)\right] \end{cases} \tag{9.12}$$

$$\begin{cases} A' = i_q(0_-) \\ B' = \left[-\frac{r}{L_q} \cdot i_q(0_-) - \frac{\omega_e \psi_f}{L_q} + \frac{i_q(0_-)}{L_d r} - \frac{\omega_e L_d}{L_q}\right] \\ C' = -\frac{\omega\psi_f r}{L_d L_q} + \frac{\omega r}{L_q} \cdot i_d(0_-) \end{cases} \tag{9.13}$$

i_d and i_q can be obtained as

$$\begin{cases} i_d(s)=A\cdot\frac{s}{(s-s_1)(s-s_2)}+B\cdot\frac{1}{(s-s_1)(s-s_2)}+C\cdot\frac{1}{s(s-s_1)(s-s_2)} \\ i_q(s)=A'\cdot\frac{s}{(s-s_1)(s-s_2)}+B'\cdot\frac{1}{(s-s_1)(s-s_2)}+C'\cdot\frac{1}{s(s-s_1)(s-s_2)} \end{cases} \tag{9.14}$$

$$\begin{cases} i_d(t)=\frac{A}{\sqrt{b^2-a^2}}\cdot\left[\begin{array}{r}-ae^{-at}\sin\left(\sqrt{b^2-a^2}\cdot t\right)\\ +e^{-at}\left(\sqrt{b^2-a^2}\right)\cdot\cos\left(\sqrt{b^2-a^2}\cdot t\right)\end{array}\right]+\frac{B}{\sqrt{b^2-a^2}}\cdot\left[e^{-at}\sin\left(\sqrt{b^2-a^2}\cdot t\right)\right] \\ \quad +C\cdot\left[1-\frac{1}{\sqrt{b^2-a^2}}\cdot e^{-at}\sin\left(\begin{array}{r}\sqrt{b^2-a^2}\cdot t\\ +\arctan\left(\frac{\sqrt{b^2-a^2}}{a}\right)\end{array}\right)\right] \\ i_q(t)=\frac{A'}{\sqrt{b^2-a^2}}\cdot\left[\begin{array}{r}-ae^{-at}\sin\left(\sqrt{b^2-a^2}\cdot t\right)\\ +e^{-at}\left(\sqrt{b^2-a^2}\right)\cdot\cos\left(\sqrt{b^2-a^2}\cdot t\right)\end{array}\right]+\frac{B'}{\sqrt{b^2-a^2}}\cdot\left[e^{-at}\sin\left(\sqrt{b^2-a^2}\cdot t\right)\right] \\ \quad +C'\cdot\left[1-\frac{1}{\sqrt{b^2-a^2}}\cdot e^{-at}\sin\left(\begin{array}{r}\sqrt{b^2-a^2}\cdot t\\ +\arctan\left(\frac{\sqrt{b^2-a^2}}{a}\right)\end{array}\right)\right] \end{cases} \tag{9.15}$$

The condition dq-Axis current initial value is not zero and the condition that dq-axis current initial value is zero have the same final steady-state values.

By the above expression we can also see, the three-phase transient short-circuit process is related to the inductance, the resistance and the flux linkage and other parameters of the motor, and also, related to the i_d, i_q initial state, of which the process is more complex, there are more influenced dynamic parameters. In the actual engineering design, the complete system response curve can be drawing by computer solving. So not only the dynamic process of the known parameters' motor can be calculated fast and the risk of demagnetization can be assessed, but also the effect to the transient short-circuit process and demagnetization current under different i_d, i_q, ψ_f and other parameters can be compared.

9.3 Transient Short-Circuit Simulation Analysis Based on the Actual Operation Condition

We have analyzed the three-phase transient short-circuit in the last chapter, which gives a analytical expression of i_d, i_q short circuit current. From the expression, it can be found that the changing process of the transient short-circuit is related to motor dq-axis inductance, permanent magnet flux and other motor parameters, and also will be effected by the speed and the initial value of $i_d i_q$ current at the moment of short-circuit state. Ignore the magnetic saturation, and assume that the motor paraments do not change in this process. The transient short-circuit time is very

short during the actual vehicle moving, considering the vehicle inertia and other factors, the simulation process can be approximated that the motor speed is constant before and after the short circuit. The operating condition at the moment of short-circuit determine the initial value of $i_d i_q$ current. Next, combining the electric vehicle common conditions, the three-phase short-circuit transient current will be simulated.

MTPA (maximum torque current ratio) of Electric vehicle PMSM is achieved by vector control. During the actual using, regardless of the flux weakening region or the non flux weakening region, the basic principle of motor control algorithm is realizing MTPA control by adjusting the $i_d i_q$ current ratio to increase the magnetic reluctance torque. PMSM torque equation is:

$$T_e = 1.5 \times P_n \times \left[\psi_f i_q + (L_d - L_q) i_d i_q\right] \tag{9.16}$$

Motor system working conditions is related to the requirement of the electric vehicle's dynamic performance closely. And the requirements of hybrid electric vehicles and pure electric vehicle are very different [6]. For embedded PMSM, usually have:

(1) Drive motor converts electrical power into mechanical energy to provide a driving force. Positive torque is corresponding to the vehicle's acceleration and climbing condition, and the q-axis current is positive, and d-axis current is negative, so the motor output torque is positive. Figure 9.2 shows, along with the MTPA curve, i_d increases, i_d decreases, positive torque increases.
(2) Q-axis current is negative, d-axis current is also negative, the motor output torque is negative, which is corresponding to power generating, braking energy recovery and other conditions. Figure 9.2 shows, i_d and i_d both increase, negative toque increase.

Use MTPA to simulate the changing process of the $i_d i_q$ current at the moment of transient short-circuit. The parameters of the star-connection motor used for simulating and testing are as follow.

Under motor system follow-up working conditions, which is without load ($i_d = 0$, $i_q = 0$), compare the short-circuit current at 1000, 2000, 3000, 4000 rpm, as shown in Fig. 9.3.

Compare the transient short-circuit current of different working condition at 1000 rpm. There are low-speed accelerating condition,i_q = 200 A, i_d = −100 A (142 Nm), low-speed climbing condition, i_q = 300 A, i_d = −250 A (291 Nm), low-speed braking energy recovery, i_q = −200 A, i_d = −100 A (−142 Nm), low-speed emergency braking, i_q = −300 A, i_d = −250 A (−296 Nm). Compare the transient short-circuit current of high-speed accelerating and high-speed braking energy recovery simultaneously (Figs. 9.4 and 9.5).

From the above simulation we can see that:

(1) At the different speed, without load short-circuit, with the higher speed, the more oscillation periods of *dq*-axis current appear. But the transient process

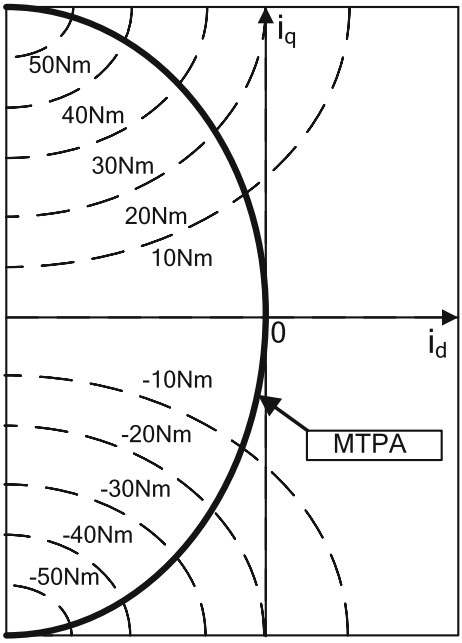

Fig. 9.2 MTPA stator current vector trajectory

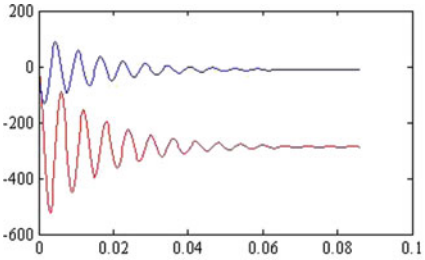

(a) 1000rpm on-load transient short-circuit current

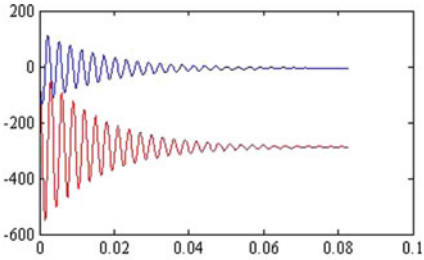

(b) 2000rpm on-load transient short-circuit current

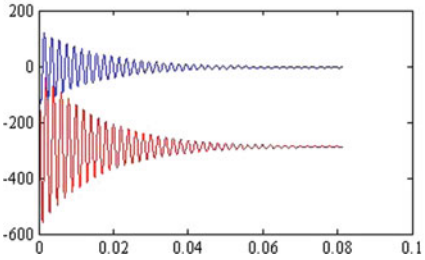

(c) 3000rpmon-load transient short-circuit current

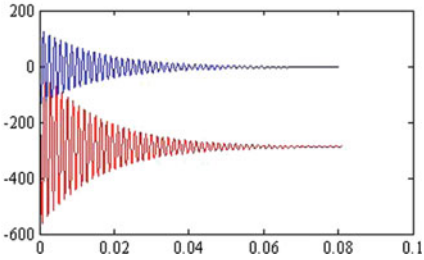

(d) 1000rpm on-load transient short-circuit current

Fig. 9.3 Transient short-circuit current simulation charts at different speed

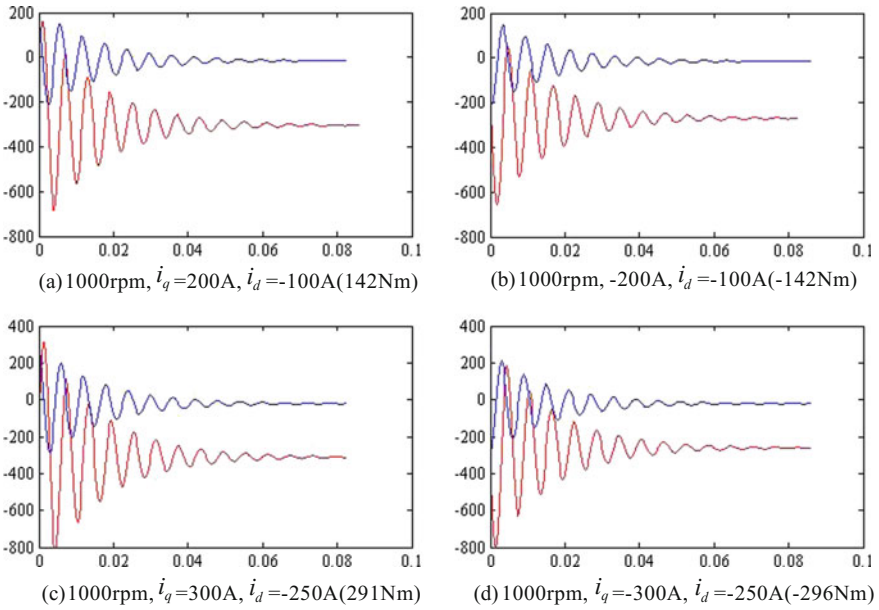

Fig. 9.4 Transient short-circuit current simulation charts at different torque

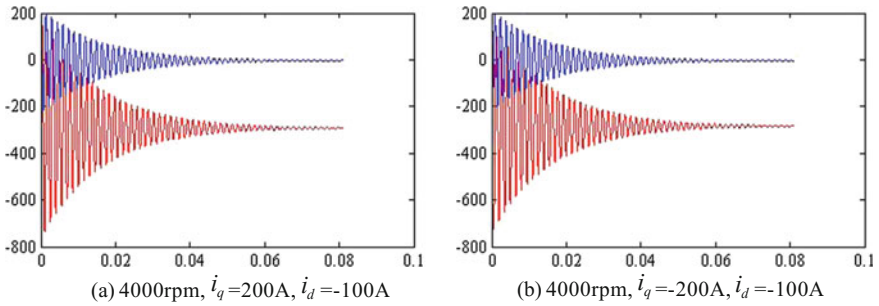

Fig. 9.5 Transient short-circuit current simulation charts at high speed

time is almost the same, the maximum demagnetization-current is almost the same too.

(2) At the same speed, with load short-circuit, regardless of driving or generating condition, with the load increasing, the demagnetization-current increases, the transient process time is almost the same.

(3) Under the same load, at different speed, with the higher speed, the demagnetization-current increases, and the more the oscillation periods appear.

9.4 Test Platform Design and Test Results Analyze

In order to verify the correctness of the analysis of PMSM transient three-phase short-circuit model theory in Chap. 2, and support the simulation in Chap. 3, this paper has completed the design of transient short-circuit test platform and the transient short-circuit test on the test platform. The unit under test (UUT) is a C-level hybrid vehicle permanent magnet synchronous motor (IPMSM). The parameters of the UUT are shown in Table 9.1, in Chap. 3.

By the above two chapters' analyzing we know the process of transient short-circuit is very complex and short. Transient current shock will make the motor torque shock and also has some destructive effect. So we need to consider the high response speed and stability to resist the impact of destruction during test platform designing.

Figure 9.6 shows the test platform, which includes dynamometer, battery simulator, elastic shaft, torque sensor, resolver and position acquisition devices, *dq*-axis current calculating unit, the tested motor and inverter, execution unit of three-phase transient short-circuit. The dynamometer as the test load should be set in speed mode during the test and the speed can be changed. The tested motor and inverter are running in torque mode by controlling the inverter's *dq*-axis current to change the output torque. A flexible coupling is installed between the tested motor and the dynamometer for eliminating the shock of the system running speed caused by the transient short-circuit torque. Compared to the tested motor, a larger inertia dynamometer is selected, in order to reduce the effect of the shock to the system stability.

The three-phase transient short-circuit execution unit mainly contains a high-power IGBT and its drive hardware circuit. The three-phase synchronous short-circuit process is triggered by hardware. The current and the position signal acquisition unit is consist of several high-response, high-precision sensors. The current and the angle signal is delivered to the *dq*-axis current calculation unit in real time, of which the output *dq*-axis current operation rate is 50 kHz. The tested

Table 9.1 The parameters of PMSM tested unit

Parameter	Value
Nominal voltage U_N/V	360
Nominal power P_N/kW	30
Nominal torque T_N/Nm	160
Peak torque T_P/Nm	320
Nominal speed n/rpm	1800
Maximum voltage n_{max}/Nm	4200
Phase resistance R_s/mΩ	13
d-axis inductance L_d/mH	14
q-axis inductance L_q/mH	30
Pole pairs p	10
Flux linkage ψ/Wb	0.456

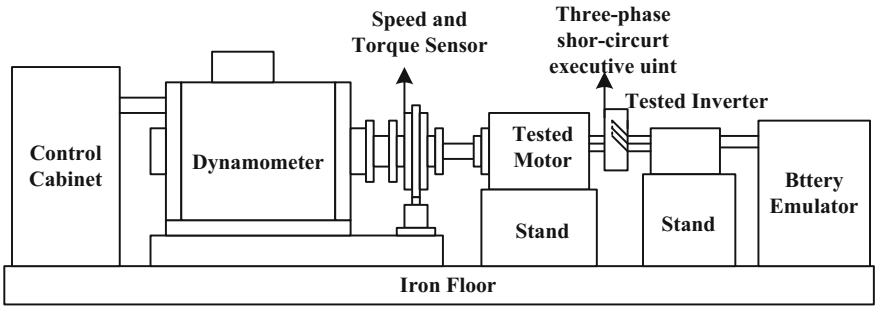

Fig. 9.6 The structure of the torque fluctuation detection system

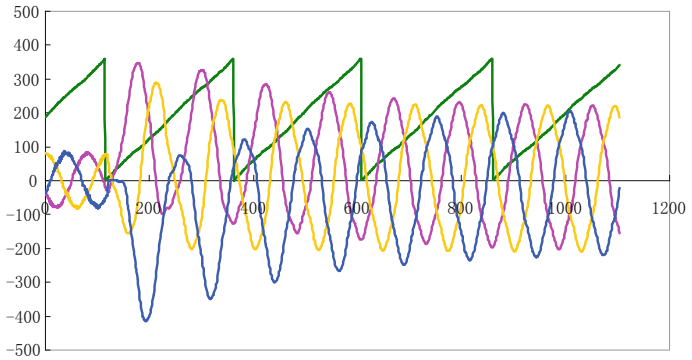

Fig. 9.7 Phase current waveform and the motor resolver position signal waveform after transient short-circuit

inverter must have over-current protection to prevent the IGBT over burning caused by the over-current in the process of the transient short-circuit.

The dynamometer is set to 1000 rpm, Fig. 9.7 is the phase current waveform and the motor resolver position signal waveform during transient short-circuit. The pole pairs of the resolver is the half of the tested motor's. The current has a great shock in the process of short-circuit, but the resolver signal is linear well, which proves the speed of the test system has no significant change during the shock, and the actual speed is consistent with simulation conditions before and after the transient short-circuit. As the current and rotor position is known, the *dq*-axis current can be calculated by Clark park in real time.

In this paper, in order to verify the correctness of the theoretical analysis and compare the simulated date and the actual test data, the following three conditions have be selected, 1000 rpm @56 Nm ($i_d = -35$ A, $i_q = 95$ A), 2000 rpm

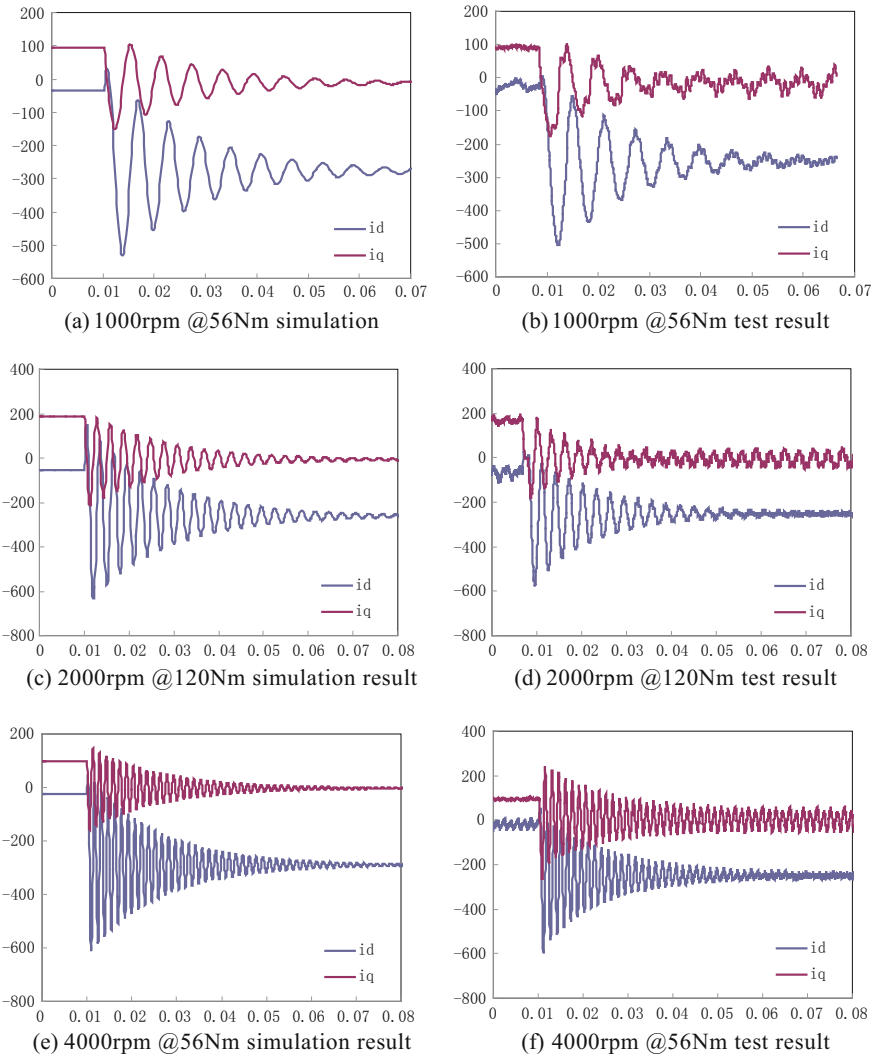

(a) 1000rpm @56Nm simulation
(b) 1000rpm @56Nm test result
(c) 2000rpm @120Nm simulation result
(d) 2000rpm @120Nm test result
(e) 4000rpm @56Nm simulation result
(f) 4000rpm @56Nm test result

Fig. 9.8 The comparison charts of the simulation results and the test results under different conditions

@120 Nm (i_d = −55 A, i_q = 195 A), 4000 rpm @56 Nm (i_d = −35 A, i_q = 95 A). The comparison charts of the simulation results and the test results under different conditions is shown in Fig. 9.8.

By comparing the simulated waveforms and the measured waveform of the above three conditions, the consistency of simulated and actual i_d, i_q current

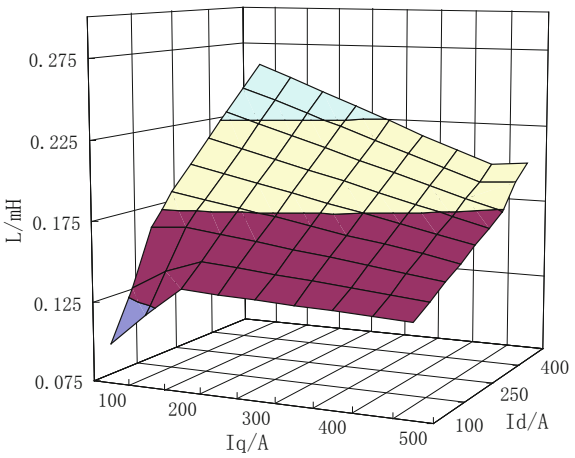

Fig. 9.9 Inductance variation curve with i_d, i_q

transient response is very high, the simulated steady-state time and the oscillation process are very consistent with the actual situation, and the maximum instantaneous value of the negative i_d current is also consistent basically. In these three conditions, the maximum simulation values of the simulation are: −522.4, −616.2, −613.7 A, the maximum measured values are: −499.8, −597.7, −600 A. The deviation of the maximum demagnetization current is within 5%. The motor after the test has no abnormal changes of mechanical and electrical characteristics. There is no demagnetization phenomenon after confirming the back EMF of the motor without load.

Next we will analyze the reason for the deviation of the simulation and the measurement, we can find that even the short-circuit process has been steady, the current also has obvious oscillations of d, q-axis (shown in Fig. 9.8) during the actual test. There are two main reasons as follows.

(1) Since the simulation has assumed the permanent magnetic field induces a sine wave of electromotive force in the phase windings and the three-phase steady-state short-circuit current is fully sinusoidal current. But actually, in addition to the fundamental wave the induced electromotive force also contains a certain amount of harmonics, and the three-phase steady-state short-circuit current also has certain amount of harmonics, so there is current oscillation during the actual test. Non-sinusoidal induced electromotive force will have some impact on the simulation of the transient process.

(2) There is a cross-saturation effect of permanent magnet synchronous motor inductance, which the parameters of L_q, L_q, ψ_f are influenced by the current actual value of i_d, i_q, as shown in Fig. 9.9. Because the test temperature is difficult to keep constant during the test, the resistance parameters and flux parameters are also influenced by temperature. Dynamic change of motor parameter will influence both the transient state and the steady state.

9.5 Conclusion

The following conclusions can be got from this paper by analyzing an simulation.

(1) Three-phase transient short-circuit analysis is very important to PMSM. The simulation analysis based on *dq*-axis models shows that the oscillation of the *dq* transient short-circuit *dq*-axis current gradually decays to steady short-circuit condition. The $-i_d$ current during the oscillation process may cause the demagnetization of permanent magnets. Simulation method can be used for fast calculating the dynamic process with the known parameters' motor and assessing the risk of demagnetization, and also for comparing the effect to the transient short-circuit process and demagnetization current under different L_d, L_q, ψ_f and other parameters.

(2) The PMSM maximum $-i_d$ current at the time of the transient short-circuit is larger than the steady-state short-circuit. The maximum $-i_d$ current and *dq*-axis current dynamic process is related to the operating conditions (the initial value of $-i_d$,i_d) and the speed at the time of transient short-circuit. The simulation results show that a higher motor speed and a greater load will cause a greater short-circuit i_d current.

(3) The transient short-circuit test bed designed in this paper can maintain the speed stability with the transient impact during the test. And the synchronization of each channel's signal is good. The tests show *dq*-axis current transient response simulation is consistent with test results, with the exact parameters of the motor, the current simulation method is applicable to PMSM transient short-circuit analysis.

(4) The transient changes of there EMF harmonic, L_d, L_q, and ψ_f will affect the short-circuit process and the steady-state value. Nest, further analysis of transient *dq* inductance will help to analyze the dynamic process and demagnetization risk accurately.

References

1. Rosero J, Espinosa AG, Cusido J, et al (2008) Simulation and fault detection of short circuit winding in a permanent magnet synchronous machine (PMSM) by means of fourier and wavelet transform. In: Instrumentation and measurement technology conference proceedings, 2008. IMTC 2008. IEEE. IEEE, 2008, pp 411–416
2. Jie B, Huichao Z, Xiuhui D et al (2014) Steady-state characteristic analysis and application of PMSM for electric vehicle with symmetrical three-phase short-circuit. Small Spec Electr Mach 42(3):17–20
3. Hongmei L, Tao C, Hongyang Y (2013) Mechanism, diagnosis and development of demagnetization fault for PMSM in electric vehicle. Trans China Electrotech Soc 28(8): 276–284

4. Chunhong Z, Xin S, Wenming T et al (2009) Calculation and measurement of transient reactance of permanent magnet synchronous motor. Electr Eng 4:14–17
5. Eilenberger A, Schrodl M (2010) Sudden short-circuit analysis of a salient permanent magnet synchronous machine with buried magnets for traction applications. In: 14th International of power electronics and motion control conference (EPE/PEMC), 2010. IEEE, T9-117-T9-120
6. Mingming H, Xinjun G, Chenghu Z et al (2013) A novel wide speed-range driving system design for electric vehicle. Trans China Electrotech Soc 28(4):228–233